

Time resolved studies of catastrophic optical mirror damage in red-emitting laser diodes

Stella N. Elliott, Peter M. Snowton, Mathias Ziegler, Jens W. Tomm, and Ute Zeimer

Citation: *J. Appl. Phys.* **107**, 123116 (2010); doi: 10.1063/1.3437395

View online: <http://dx.doi.org/10.1063/1.3437395>

View Table of Contents: <http://jap.aip.org/resource/1/JAPIAU/v107/i12>

Published by the [American Institute of Physics](http://www.aip.org).

Related Articles

Electroluminescence from strained germanium membranes and implications for an efficient Si-compatible laser
Appl. Phys. Lett. **100**, 131112 (2012)

A weakly coupled semiconductor superlattice as a potential for a radio frequency modulated terahertz light emitter
Appl. Phys. Lett. **100**, 131104 (2012)

Quantum-dot nano-cavity lasers with Purcell-enhanced stimulated emission
Appl. Phys. Lett. **100**, 131107 (2012)

Effect of internal optical loss on the modulation bandwidth of a quantum dot laser
Appl. Phys. Lett. **100**, 131106 (2012)

Design of three-well indirect pumping terahertz quantum cascade lasers for high optical gain based on nonequilibrium Green's function analysis
Appl. Phys. Lett. **100**, 122110 (2012)

Additional information on *J. Appl. Phys.*

Journal Homepage: <http://jap.aip.org/>

Journal Information: http://jap.aip.org/about/about_the_journal

Top downloads: http://jap.aip.org/features/most_downloaded

Information for Authors: <http://jap.aip.org/authors>

ADVERTISEMENT



**FIND THE NEEDLE IN THE
HIRING HAYSTACK**

Post jobs and reach
thousands of hard-to-find
scientists with specific skills



<http://careers.physicstoday.org/post.cfm> **physicstodayJOBS**

Time resolved studies of catastrophic optical mirror damage in red-emitting laser diodes

Stella N. Elliott,^{1,a)} Peter M. Smowton,¹ Mathias Ziegler,² Jens W. Tømm,² and Ute Zeimer³

¹*Cardiff School of Physics and Astronomy, Cardiff University, The Parade, Cardiff CF24 3AA, United Kingdom*

²*Max-Born-Institut, Max-Born-Str. 2 A, 12489 Berlin, Germany*

³*Ferdinand-Braun-Institut fuer Hoechstfrequenztechnik, Gustav-Kirchhoff-Str. 4, 12489 Berlin, Germany*

(Received 3 January 2010; accepted 5 May 2010; published online 25 June 2010)

We have observed the changing light intensity during catastrophic optical mirror damage (COMD) on the timescale of tens of nanoseconds using red-emitting AlGaInP quantum well based laser diodes. Using as-cleaved facets and this material system, which is susceptible to COMD, we recorded the drop in light intensity and the area of damage to the facet, as a function of current, for single, high current pulses. We found that in the current range up to 40 A, the total COMD process up to the drop of light intensity to nonlasing levels takes place on a timescale of hundreds of nanoseconds, approaching a limiting value of 200 ns, and that the measured area of facet damage showed a clear increase with drive current. Using a straightforward thermal model, we propose an explanation for the limiting time at high currents and the relationship between the time to COMD and the area of damaged facet material. © 2010 American Institute of Physics.

[doi:10.1063/1.3437395]

I. INTRODUCTION

Catastrophic optical mirror damage (COMD) remains a limiting factor in the increasing drive for high power semiconductor diode lasers. Much research effort continues to be invested to lead to technological improvements that will both raise the power levels attainable and detect the imminence of COMD before it actually occurs, thus preventing damage.

The total COMD process¹⁻⁴ consists of an initial facet temperature rise, followed by thermal runaway, facet melting, propagation of melt front leading to dark lines, and drop of lasing power and is thought to take place on a timescale of the order of hundreds of nanoseconds, with some evidence for this from previous studies that used 2 μ s pulses and a thermocamera to observe the COMD on a microsecond timescale.⁵ All time studies to date have been carried out at microsecond resolution^{6,7} whereas here we apply single, short, high current pulses, observing the COMD process using a fast photodiode to shorten the time resolution to tens of nanoseconds. We find that although the time to COMD (from the start of current to the optical power drop associated with catastrophic damage) gradually shortens as the optical power increases, it remains finite even at very high powers, tending to a limiting time of about 200 ns for these devices, over the current range studied. We propose a physical explanation for the limiting, constant time.

Many facet treatment processes exist to protect facets and increase the power density a laser can sustain before COMD occurs. In order to investigate the physics of COMD itself, we used red-emitting AlGaInP based lasers, which are known to be susceptible to COMD, with as-cleaved facets. Thus, any effects seen were due to the intrinsic properties of

the facets themselves with no change due to passivation, nonabsorbing mirrors, or coatings, which will improve the performance but obscure the physics. The devices we used, originally designed for medium power optical storage use, provided large regions of damage and thus very clear and unambiguous results. We used 50 μ m oxide isolated stripe lasers and applied single, square current pulses of up to 40 A for 1000 ns only, to a fresh device each time, monitoring the current pulse and the light output with a photodiode synchronized to the current pulse trigger, as a function of time. We recorded the nearfield and the appearance of the facet using a high quality optical microscope before and after the current pulse and carried out scanning electron microscopy on selected devices. The facet images confirmed severe damage, which was also clearly indicated by the decrease in the amplitude of the nearfields. We obtained the time to COMD from the photodiode pulses and the damaged facet area from the micrographs, both as a function of current. We found that as current increased, not only did the time to COMD shorten to a limiting value but the measured area of facet damage increased steadily. In the current traces, we observed kinks that followed closely after the drop in light power. Such kinks have previously been suggested as a possible signal to instigate a damage limitation process.⁷

Several mechanisms have been suggested for facet heating, including optical reabsorption⁸ and surface currents on the facet.^{9,10} The contribution of any particular process will depend on how far away from threshold the laser is being operated and the condition of the facet, surface defect sites or oxidation, for example, will cause nonradiative recombination of injected or photogenerated carriers. The effects of facet heating will be moderated if facet passivation and coatings, current blocking regions, or nonabsorbing mirrors are used.

^{a)}Electronic mail: spxse@cf.ac.uk.

The time to COMD has been modeled¹ but has not previously been experimentally investigated on the timescale of the thermal runaway. The chemical or thermal processes that take place on the facet after thermal runaway has commenced are not well known, making it difficult to obtain good agreement between quantitative modeling and experiment¹¹ and increasingly sophisticated approaches are being adopted.¹² There are numerous observations of propagating melt fronts¹⁻⁴ inside the device. We looked for a simple explanation that linked the limiting time and the large amount of facet damage observed in these devices.

We propose the following explanation of the finite limit of the time to COMD. The total time to COMD (t_{COMD}) is the sum of the time for the temperature to rise (t_{rise}) and the time to melt (t_{melt}). t_{rise} is dominated by the relatively slow facet temperature rise to the critical temperature at which thermal runaway occurs, the time for runaway being negligible in comparison. The rate of facet temperature rise is proportional to the optical power, giving t_{rise} approximately inversely proportional to current and tending to zero at high currents. Both t_{melt} and the absorbed optical energy required for melting are proportional to the mass of melted material. The mass melted and energy required both increase with current, and would tend to increase t_{melt} , but the power available for absorption also rises, which tends to decrease t_{melt} . These effects cancel over the current range used, leading to a constant t_{melt} . Thus, if

$$t_{\text{COMD}} = t_{\text{rise}} + t_{\text{melt}}, \quad (1)$$

$$t_{\text{COMD}} \rightarrow 0 + \text{const}, \quad (2)$$

as current increases.

II. SAMPLE AND EXPERIMENTAL DETAILS

The active region consisted of three 5 nm compressively strained GaInP quantum wells (QWs) separated by lattice matched AlGaInP barrier regions (with an Al fraction of 0.5) in a waveguide region of the same composition. The total core width was 0.23 μm . The cladding region consisted of lattice matched AlGaInP (Al fraction 0.7) with 0.25 μm AlGaInP (Al fraction 0.5) mode expansion layers inserted in the cladding on each side.¹³ Etch stop GaInP layers were grown on both sides (to preserve the symmetry of the structure) about 0.4 μm from the center of the structure. The cladding layers were doped with Si (n) and Mg (p). The structures were red emitters with wavelengths of between 654–658 nm, depending on device length. Identical 50 μm oxide isolated stripe devices were mounted p-side up on copper heat sinks on transistor headers. The electrical contacts consisted of multiple gold wires (p) and the copper heat sink (n). The mounting and all contacts were made using Epotek conductive epoxy. The chip dimensions were 300 μm wide and 120 μm deep with a cavity length of 1000 μm . This mounting was adequate heat sinking for the short times of the current pulses used. (A characteristic length for conduction of heat for this material, given by $\sqrt{\kappa t}$, where κ is the thermal diffusivity and t is the pulse length, is of the order of 1–2 μm .)

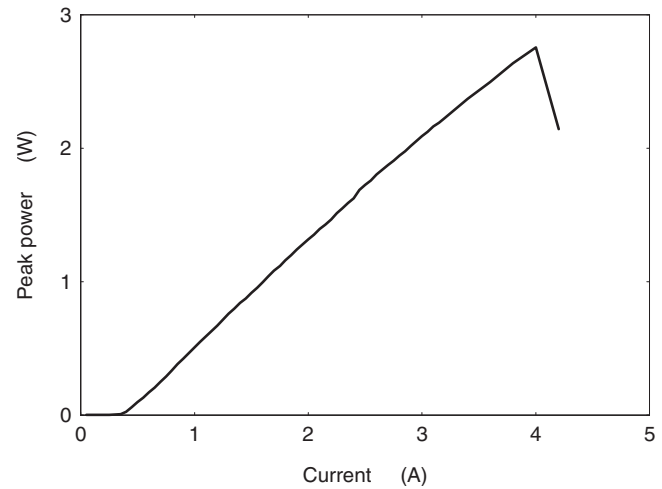


FIG. 1. Typical power-current characteristic of a 750 μm device taken right up to COMD under repeated pulse conditions.

The devices used in the single pulse experiment were individually characterized using repeated pulse conditions (400 ns, 0.0004 duty cycle) at very low currents and had a typical threshold of 0.5 A. High power behavior from a similar device, also operated pulsed, from the same wafer is shown in Fig. 1. After characterization the transistor headers were soldered directly to the output of a Picolas (LDP-V 50–100 V3) pulse generator. The time constant of the pulse generator, device and current sensing circuitry was measured to be 13 (± 1) ns. The pulse generator was mounted directly under a high quality Leica DM4000M optical microscope so that the nearfields and facets could be imaged (using a Leica DFC320 camera) without moving the device. Neutral density filters were used to prevent saturation when the nearfields and light pulses were recorded. The photodiode (Siemens BPX65) was inserted between the device and the microscope at a position of maximum intensity in the farfield, capturing a small but fixed proportion of the total output power, regardless of the exact position of the damage. The consistency of the measured times gave additional confidence the setup used monitored a representative fraction of the light output. The time constant for the photodiode and associated electronic data capture circuitry was 18 (± 2) ns.

We subjected the lasers to square current pulses of 1000 ns length, at increasing currents of up to 40 A, using a fresh device for each pulse. This should be long enough at most currents used for COMD to occur. The light pulses emitted from the lasers were monitored by the photodiode and recorded using an oscilloscope synchronized to the current pulse trigger, together with the current pulses. The facets and nearfields were imaged before and after the pulse using the microscope. The nearfields were obtained using electroluminescence at pulsed (12 ns), very low currents (about 1 A) at a very low repetition rate in order not to age the device in any significant way. We obtained the time to COMD, the area of facet damage, and the time of any current transients from this data. In a supplementary investigation, one device was subject to repeated identical 10 A, 1000 ns pulses to provide additional confirmation of the permanent nature of the damage to the device after the first pulse. A large drop in

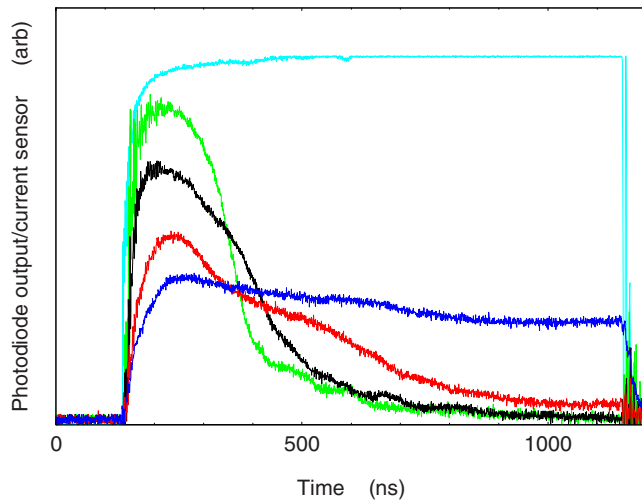


FIG. 2. (Color online) Examples of photodiode traces of increasing amplitude as a function of current for 5, 10, 20, and 40 A, showing the drop in light intensity for the higher currents, together with an example of a current trace (top trace).

light intensity was observed between the first and second current pulses, followed by much smaller changes in subsequent pulses.

III. SHORT PULSE EXPERIMENTAL DATA

For currents of 8 A and above, the photodiode signal showed a drop in light intensity to nonlasing levels during the pulse (Fig. 2). Facet damage was clearly visible in optical micrographs (illuminated with white light) of the facets as a darkened, nonuniform area of the active region in the area beneath the stripe [Fig. 3(b)]. If low current, short pulses were then applied to the damaged device, the damaged region could be seen as a nonluminescent area in the center of the red, nearfield electroluminescence. These darkened areas were not observed in images taken of fresh devices before the current pulse was applied, in which the nearfield electroluminescence was uniformly distributed [Fig. 3(a)].

From the photodiode traces, we measured the time for the power to drop to half its peak value, the time to COMD (Fig. 4). We found that as current increased, the time to COMD shortened but did not tend to zero, approaching instead a limiting value of about 200 ns over the current range used.

In order to measure the area of damaged facet material, we obtained optical micrographs of unilluminated facets, displaying the damaged region by applying repeated low energy current pulses (as described above). This resulted in images of the electroluminescence emitted by the facet. The damaged areas were the dark, nonemitting regions in the center of the electroluminescence, and were measured by superimposing a calibrated grid (Fig. 5).

The damage covered an area that increased with current (Fig. 6).

The nanosecond timescale of these measurements enabled us to observe a kink in the current trace that followed the drop in light level (Fig. 7). These kinks were only observed at currents above the threshold for facet damage, and in these red-emitting devices with uncoated facets. In some

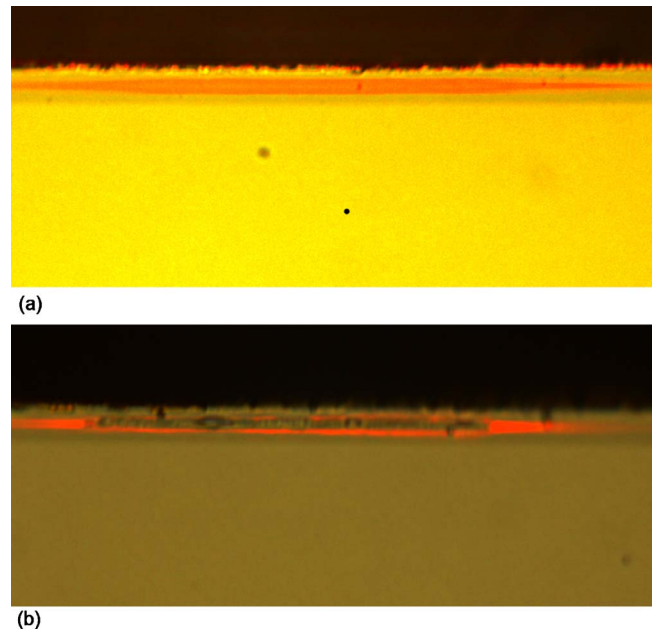


FIG. 3. (Color online) Optical micrographs of facets. The active region is at the top of the p-side up mounted device. The condition of the facet is shown in two ways: the facet is illuminated with white light and red electroluminescence is produced by low level current pulses. (a) A pristine facet characterized by uniform appearance and electroluminescence. (b) Facet damage was clearly visible in this device after a 1 μ s, 15 A current pulse. Electroluminescence is seen in the area surrounding the damage, which is the darkened, nonradiative area in the center of the active region.

traces there appeared to be more than one drop in the light level, which was often followed by a second current kink. Previous work has suggested using such transients (albeit measured with microsecond time resolution) to activate circuitry to cut the laser diode power supply, preventing further damage, and prolonging the life of the laser.⁷ We find that for our devices the kink occurs within tenths of microseconds of the initial power drop signaling the onset of damage (at our operating conditions, above normal working currents). If this was the case at lower currents too it would indicate the short timescale on which such protective circuitry would have to

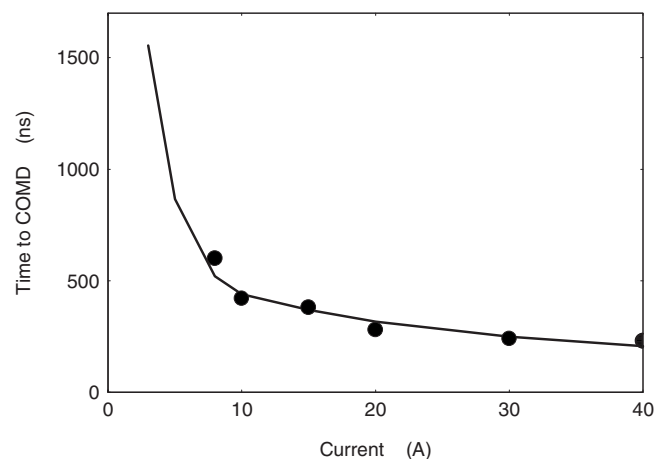


FIG. 4. Measured time to COMD (from start of current pulse to half power) for the devices as a function of pulse current (points). This time approaches a constant, limiting value of about 200 ns, asymptotically, as current increases. Calculated (line) time to COMD using the thermal model detailed later in the paper.

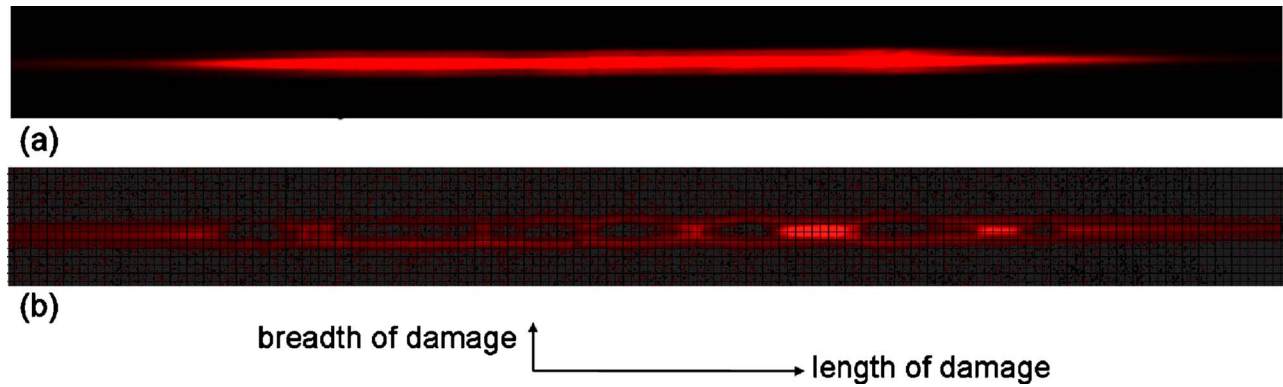


FIG. 5. (Color online) (a) Image of the nearfield emission from the facet of a device before aging with a 30 A, 1000 ns current pulse. (b) Image of the same device after application of the pulse. The damage can be seen as the dark regions surrounded by electroluminescence. The image has been brightened due to the low remaining light levels. The superimposed grid enables measurement of facet area damaged at COMD. The facet is not illuminated by the microscope and cannot be seen. Each grid square is 10×10 pixels ($0.68 \times 0.68 \mu\text{m}$).

operate. The microscopic origins of these electrical transients remain unclear. The current kinks could signal a new event such as the initiation of another area of facet damage or of a branch in the molten tracks, causing a change in conductivity of the facet or interior of the device because of a change in phase, such as melting or segregation of the components of the alloys. The cathodoluminescence image (Fig. 9) of the melt fronts suggest portions originating at different points on the facet either travel at different speeds or are initiated at different times. The measured time constants of the current rise time and the current kink were very similar (13 ± 1 ns) implying the process took place on a timescale of this order or shorter.

IV. TIME TO COMD

The COMD sequence of events consists of a relatively slow and comparatively small facet temperature rise followed by a large, runaway temperature rise (of negligible duration in comparison). This is followed by facet damage and propagation of molten regions until sufficient damage has occurred to prevent further lasing. In order to evaluate the time to COMD (t_{COMD}), the time for the temperature to

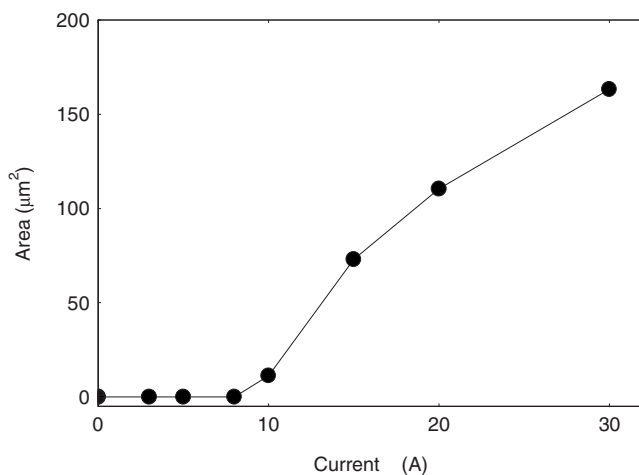


FIG. 6. Measured area of damage on facet.

rise (t_{rise}) and the time for the facet to melt and defect regions to form in the interior of the device (t_{melt}) must be determined

$$t_{\text{COMD}} = t_{\text{rise}} + t_{\text{melt}}.$$

Both t_{rise} and t_{melt} would be expected to shorten as the availability of absorbed power increases with current, but we suggest t_{melt} depends also on the area of facet damage and hence volume of melted material inside the device, which increase with absorbed power, and that this is why the time to COMD remains longer than expected.

To model the measured t_{COMD} , we assumed the heating mechanism was reabsorbed optical power, and used the following equations:

$$t_{\text{rise}} = k_1/P_{\text{opt}}, \quad (3)$$

$$t_{\text{melt}} = k_2 A/P_{\text{opt}}, \quad (4)$$

where P_{opt} is the optical power, A is the damaged facet area, and these and the times are functions of pumping current. k_1 and k_2 are constants and were adjusted until a fit was obtained to the measured values of t_{COMD} (Fig. 4). The values

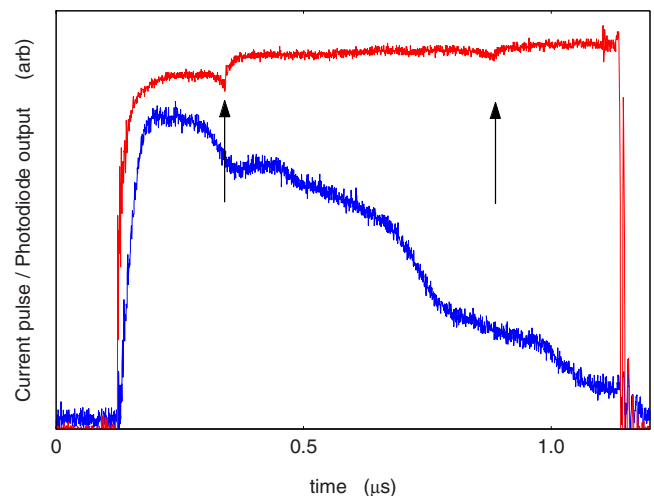


FIG. 7. (Color online) Traces for photodiode output (lower, blue trace) and current (upper, red trace) for a device pulsed at 8 A. The kinks in the current traces (marked with arrows) always occurred after a drop in light level.

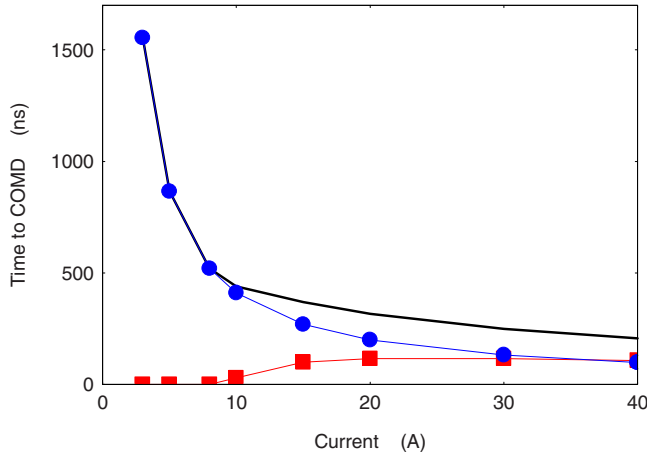


FIG. 8. (Color online) Calculated time for temperature of the facet to rise to thermal runaway (blue circles, upper trace) and time for the quantity of damaged material, based on measured areas of facet damage, to melt (red squares, lower trace). The total time to COMD, the sum of these, is shown by the black line (shown also in Fig. 3, with the measured values).

obtained for k_1 and k_2 were 3.75×10^{-6} J and 2.00×10^{-8} J/ μm^2 , respectively.

Curves for t_{rise} and t_{melt} and their sum are plotted in Fig. 8 as a function of the magnitude of the current pulse.

We now consider a possible physical basis for the values of k_1 and k_2 using simple energy arguments. The temperature (T) of a mass of facet material rises through ΔT , absorbing a quantity of energy $m_{\text{rise}}c\Delta T$ (mass \times specific heat \times temperature change). We calculate t_{rise} from the energy absorbed during the slow temperature rise up to the point of thermal runaway. We assume thermal runaway can be neglected since it takes only a very small fraction of the time for the temperature to rise to the point of COMD and also the final temperature attained by the facet is not well known experimentally. After thermal runaway and facet damage have taken place molten regions propagate through the interior of the device until there is insufficient optical intensity produced by the remaining undamaged active region to cause further melting. The molten material absorbs heat $m_{\text{melt}}L$ (mass \times latent heat of fusion).

Thus, for facet temperature rise we have

$$P_{\text{opt}} \times \text{fraction of power absorbed} \times t_{\text{rise}} = m_{\text{rise}}c\Delta T, \quad (5)$$

$$t_{\text{rise}} = m_{\text{rise}}c\Delta T / (\text{fraction of optical power absorbed}) \times 1/P_{\text{opt}}. \quad (6)$$

We, therefore, attribute the following physical quantities to k_1 in Eq. (3):

$$k_1 = m_{\text{rise}}c\Delta T / (\text{fraction of optical power absorbed}). \quad (7)$$

Using energy arguments for the propagating melt front, we have

$$P_{\text{opt}} \times t_{\text{melt}} = m_{\text{melt}} \times L, \quad (8)$$

$$t_{\text{melt}} = L \times m_{\text{melt}} \times 1/P_{\text{opt}}. \quad (9)$$

We estimate the volume of molten material by $v t A$, where v is the propagation velocity of the melt front during the pulse, of length t (1 μs).

$$t_{\text{melt}} = L_v v t A \times 1/P_{\text{opt}}, \quad (10)$$

giving for k_2 in Eq. (4)

$$k_2 = L_v v t, \quad (11)$$

where L_v is the latent heat of fusion per unit volume.

We estimated values for these physical constants from the literature and from subsidiary experiments, and found they are consistent with the values of k_1 and k_2 obtained from fitting to the measured time to COMD data. These estimates are discussed now and are summarized in Table I.

Quantities that contribute to k_1 are the mass of facet material heated, the specific heat capacity, the temperature change, and the fraction of optical power absorbed. Since the nearfield is reasonably uniform at low powers [Fig. 3(a)] the heating will initially occur uniformly across the facet. We took the heated facet volume to be the length under the stripe multiplied by the calculated $1/e^2$ power density breadth (length and breadth defined in Fig. 5) multiplied by a depth inside the device of the order of $\sqrt{(\kappa t)}$, giving a heated facet volume of approximately 50 μm^3 and the corresponding mass, m_{rise} . Since the $\sqrt{(\kappa t)}$ depth into the active region is also the distance over which light is absorbed, and was used to calculate the fraction of power absorbed ($I/I_0 = e^{-\Gamma x}$), changing the $\sqrt{(\kappa t)}$ depth results in no net change in k_1 . Based on modal absorption measured as a function of temperature we estimated that the fraction of power absorbed over a 1 μm depth could vary up to 2%. We assumed a

TABLE I. Values of data used in calculating the time to COMD.

Values for k_1	3.75×10^{-6} J
Fraction of optical power absorbed	0.5%
Volume of heated facet	50 μm^3
Specific heat of facet material	0.42 J/g K (linear interpolation from binaries ^a)
Facet temperature rise	200 K
Values for k_2	2.00×10^{-8} J/ μm^2
v	6 m/s
Latent heat of fusion of GaInP	3.3 kJ/cm ³ (linear interpolation of GaP and InP ^b)
Pulse length	1 μs

^aReference 14.

^bReference 15.

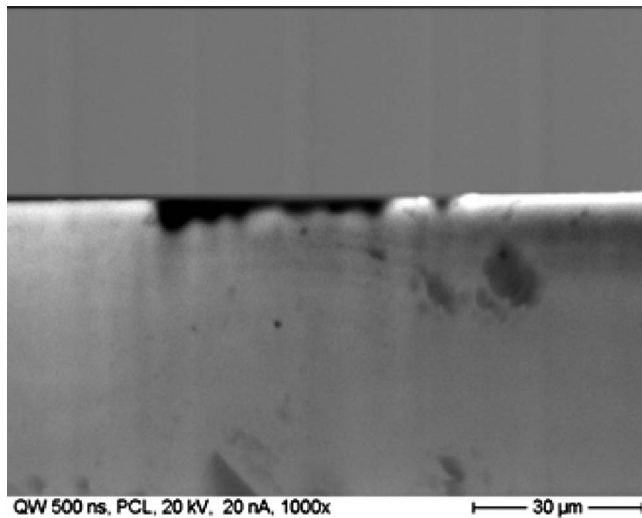


FIG. 9. Cathodoluminescence image in the plane of the active region of a device after pulsing at 10 A for 500 ns, showing dark lines propagating back from the facet into the interior of the device (at the bottom of the image). The device was mounted p-side down and the n-doped layers were removed to expose the active region. Using these lines we obtained values of the propagation velocity of the melt front for GaInP ranging between 5 and 13 m/s.

lower value for the early stage of the temperature rise, before thermal runaway, of 0.5%. With regard to the specific heat, value of c for AlGaInP was used since the facet damage extended through the epitaxial layers from the GaInP QWs into the Al_{0.5}GaInP core, which thus comprised the bulk of the heated facet material. The values for specific heat and densities were linearly interpolated from values for the binaries obtained from the literature. Finally, considering ΔT , a temperature rise of 120–140 K before thermal runaway¹⁶ has been observed in AlGaAs QW lasers, but this was averaged over the area of the QW and cladding layers covered by a 1.5 μm micro-Raman probe beam: we used a slightly higher temperature rise of 200 K.

For k_2 , we need the latent heat of fusion (again obtained by interpolation from values for the binaries in kJ/cm^3) and volume of melted material. We used a value of latent heat for GaInP, since the propagating molten region in the interior has been found to be mainly confined to the QW layers.² The melted volume was estimated by multiplying the area of facet damage, which showed a clear increase with current (Fig. 6), by the depth the melt front propagated into the device during the pulse time of 1 μs . The velocity of propagation of the melt front has been experimentally determined by several authors in GaAs based lasers, with values from 1–5 m/s^{1,3,5,17} and 10–20 m/s^{4,7} for repeated pulses or cw current. For these methods as the amount of damage increases and optical power decreases with time the velocity of the melt front was found to decrease. We obtained values ranging between 5 and 13 m/s across the facet for GaInP using a device specially prepared for cathodoluminescence from the same batch as the pulse series (Fig. 9), aged with a single 500 ns pulse at 10 A. A single short pulse allows less variation in the propagation velocity during the aging process and therefore more confidence in the values obtained. The apparent variation in velocity with position along the facet may

indicate some portions of damage starting at a later time because of a variation in intensity due to filamentation. A value of 6 m/s was used to obtain the molten volume in k_2 . Uncertainties in molten volume notwithstanding, we found that provided the molten volume increases with current (regardless of the exact relationship), a limiting, constant time is found over the current range used.

Although there are uncertainties in some of the parameters used the form and the values of the calculated time to COMD agree well with measured values as plotted in Fig. 4, suggesting this is a feasible explanation of the nature of the COMD process, compatible with the order of magnitude of the parameters involved, and that the process takes a minimum time to occur even at these high currents.

V. SUMMARY AND CONCLUSIONS

To summarize, we have observed the light intensity during COMD on the timescale of tens of nanoseconds using single, high current pulses applied to red-emitting AlGaInP QW based laser diodes. Using as-cleaved facets and this material system, which is susceptible to COMD, we were able to clearly observe and investigate the damage to the facet. We discovered that in the current range up to 40 A, the total COMD process up to the drop of light intensity to nonlasing levels takes place on a timescale of hundreds of nanoseconds, approaching a limiting value of 200 ns, and that there was a clear relationship between the measured area of facet damage and the drive current. We showed that a straightforward thermal model was consistent with the limiting time at high currents and the relationship between the time to COMD and the area of damaged facet material.

ACKNOWLEDGMENTS

We gratefully acknowledge the financial support for trans-national access of LASERLAB-EUROPE—The Integrated Initiative of European Laser Research Infrastructures II (mbi001504). S.E. thanks IQE (Europe) Ltd. and the U.K. Engineering and Physical Sciences Research Council (EPSRC) for the provision of a CASE award. Some further assistance has been provided by the EPSRC under Grant No. EP/F006683.

¹C. H. Henry, P. M. Petroff, R. A. Logan, and F. R. Merritt, *J. Appl. Phys.* **50**, 3721 (1979).

²M. B. Sanayeh, P. Brick, W. Schmid, B. Mayer, M. Müller, M. Reufer, K. Streubel, S. Schwirzke-Schaaf, J. W. Tomm, A. Danilewsky, and G. Bacher, *J. Mater. Sci.: Mater. Electron.* **19**, S155 (2008).

³O. Ueda, K. Wakao, S. Komiya, A. Yamaguchi, S. Isozumi, and I. Umebu, *J. Appl. Phys.* **58**, 3996 (1985).

⁴R. E. Mallard, R. Clayton, D. Mayer, and L. Hobbs, *J. Vac. Sci. Technol. A* **16**, 825 (1998).

⁵M. Ziegler, J. W. Tomm, D. Reeber, T. Elsaesser, U. Zeimer, H. E. Larsen, P. M. Petersen, and P. E. Andersen, *Appl. Phys. Lett.* **94**, 191101 (2009).

⁶D. R. Miftakhutdinov, I. V. Akimova, A. P. Bogatov, T. I. Gushchik, A. E. Drakin, N. V. D'yachkov, V. V. Popovichev, and A. P. Nekrasov, *Quantum Electron.* **38**, 993 (2008).

⁷J. H. Jacob, R. Petr, M. A. Jaspan, S. D. Swartz, M. T. Knapczyk, A. M. Flusberg, A. K. Chin, and I. Smilanski, *Proc. SPIE* **7198**, 719815 (2009).

⁸M. Ziegler, V. Talalaev, J. W. Tomm, T. Elsaesser, P. Ressel, B. Sumpf, and G. Erbert, *Appl. Phys. Lett.* **92**, 203506 (2008).

⁹J. W. Tomm, F. Rinner, J. Rogg, E. Thamm, C. Ribbat, R. Sellin, and D.

- Bimberg, *Proc. SPIE* **4993**, 91 (2003).
- ¹⁰W. C. Tang, H. J. Rosen, P. Vettiger, and D. J. Webb, *Appl. Phys. Lett.* **59**, 1005 (1991).
- ¹¹R. Schatz and C. G. Bethea, *J. Appl. Phys.* **76**, 2509 (1994).
- ¹²J. Mukherjee and J. G. McInerny, *IEEE J. Sel. Top. Quantum Electron.* **13**, 1180 (2007).
- ¹³S. N. Elliott, P. M. Snowton, and G. Berry, *IEE Proc.-J: Optoelectron.* **153**, 321 (2006).
- ¹⁴S. Adachi, *Properties of Semiconductor Alloys* (Wiley, Chichester, U.K., 2009).
- ¹⁵N. N. Sirota, *Semiconductors and Semimetals*, Physics of III-V Compounds Vol. 4, edited by R. K. Willardson and A. C. Beer (Academic, New York, 1968), Chap. 2.
- ¹⁶W. C. Tang, H. J. Rosen, P. Vettiger, and D. J. Webb, *Appl. Phys. Lett.* **58**, 557 (1991).
- ¹⁷B. W. Hakki and F. R. Nash, *J. Appl. Phys.* **45**, 3907 (1974).